THE JOURNAL OF PHYSICAL CHEMISTRY B

ARTICLE

pubs.acs.org/JPCB

Structural Effects of Insulin-Loading into H_{II} Mesophases Monitored by Electron Paramagnetic Resonance (EPR), Small Angle X-ray Spectroscopy (SAXS), and Attenuated Total Reflection Fourier Transform Spectroscopy (ATR-FTIR)

Tehila Mishraki,[†] Maria Francesca Ottaviani,[*,‡] Alexander I. Shames,[§] Abraham Aserin,[†] and Nissim Garti[*,†]

[†]The Ratner Chair of Chemistry, Casali Institute of Applied Chemistry, The Institute of Chemistry, The Hebrew University of Jerusalem, Edmond J. Safra Campus, Givat Ram, Jerusalem 91904, Israel

[‡]Department of Geological Sciences, Chemical and Environmental Technologies, University of Urbino, Loc. Crocicchia, Urbino 61029, Italy

[§]Department of Physics, Ben-Gurion University of the Negev, P.O. Box 653, Beer-Sheva 84105, Israel

ABSTRACT: Insulin entrapment within a monoolein-based reverse hexagonal (H_{II}) mesophase was investigated under temperature-dependent conditions at acidic (pH 3) and basic (pH 8) conditions. Studying the structure of the host H_{II} system and the interactions of insulin under temperature-dependent conditions has great impact on the enhancement of its thermal stabilization and controlled release for the purposes of transdermal delivery. Small angle X-ray spectroscopy (SAXS) measurements show that pH variation and/or insulin entrapment preserve the hexagonal structure and do not influence the lattice parameter. Attenuated total reflection Fourier transform spectroscopy (ATR-FTIR) spectra indicate that, although insulin interacts with hydroxyl groups of GMO in the interface region, it is not affected by pH variations. Hence different microenvironments within the H_{II} mesophase were monitored by a computer-aided electron paramagnetic resonance (EPR) analysis using 5-doxylstearic acid (5-DSA) as a pH-dependent probe. The microviscosity, micropolarity, order of systems, and distribution of the probes in different microenvironments were influenced by three factors: temperature, pH, and insulin solubilization. When the temperature is increased, microviscosity and order parameters decreased at both pH 3 and 8, presenting different decrease trends. It was found that, at pH 3, the protein perturbs the lipid structure while "pushing aside" the un-ionized 5-DSA probe to fit into the narrow water cylinders. At the interface region (pH 8), the probe was distributed in two differently structured environments that significantly modifies by increasing temperature. Insulin loading within the H_{II} mesophase decreased the order and microviscosity of both the microenvironments and increased their micropolarity. Finally, the EPR analysis also provides information about the unfolding/denaturation of insulin within the channel at high temperatures.

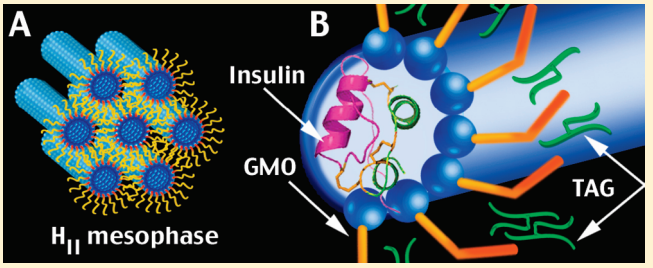

1. INTRODUCTION

Insulin is a small protein hormone that is crucial for the control of glucose metabolism and in diabetes treatment. Although insulin was discovered 90 years ago, the main route of absorption is still daily subcutaneous (sc) injection, which is associated with side effects such as pain, itching, allergy, and even lipodystrophy upon chronic administration to the same injection site.[1−3] Furthermore, good glycemic normalization cannot be reached by the traditional sc insulin preparations.[4] Various attempts to deliver insulin through oral, nasal, pulmonary, and rectal routes have been made. However, all of the mentioned trials had difficulties in overcoming the readily digested insulin, its deactivation by proteases found throughout the gastrointestinal tract (GIT), and its low transfer through the cell membrane of the epithelium lining the GIT.[5−7] Thus, transdermal delivery seems to be an attractive method to overcome the mentioned obstacles. Yet, the skin is impermeable to large hydrophilic polypeptides such as insulin. Consequently, different external methods have been tested to improve transdermal transfer, such as iontophoresis,[8] low-frequency ultrasound (phonophoresis),[9] and drug-carrier agents.[10] The limitations and the difficulty in crossing the barrier of the stratum corneum (SC) by various molecules can be addressed and partially overcome using penetration enhancers, compounds that increase the diffusion coefficient of the drug through the SC.[11]

An additional obstacle that complicates insulin delivery is its poor stability with a tendency to aggregate and denature upon exposure to strong shear forces, hydrophobic surfaces, high temperatures, or incompatible solvents. The fastidious nature of

Received: February 10, 2011
Revised: May 17, 2011
Published: May 18, 2011

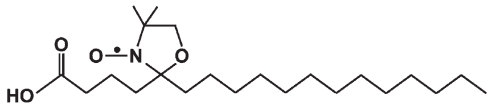

Figure 1. Chemical structure of 5-doxylstearic acid (5-DSA).

insulin necessitates development of stability-enhancing delivery devices.

Lyotropic liquid crystals (LLC), and in particular reverse hexagonal mesophase (H_{II}), are good candidates as alternative delivery vehicles for a wide range of pharmaceuticals (both hydrophilic and hydrophobic drugs). H_{II} mesophases are formed by water and glycerol monofatty-acid esters (monoglycerides). These structures can accommodate biologically active molecules, either within the aqueous domains, composed of dense packed, infinitely long, and straight water-filled rods, or by direct interaction within the lipid hydrophobic moieties, radially oriented outward from the centers of the water rods.[12−15]

Owing to these properties, the H_{II} mesophases can be specifically used to solubilize and transport therapeutic peptides and proteins by both oral and transdermal routes. The components of the proposed hexagonal carriers (GMO and TAG) also act as chemical penetration enhancers and would assist the drug to overcome the SC barrier.

In our previous reports, a model protein (lysozyme, LSZ) was incorporated within the H_{II} mesophase revealing improvement in the conformational stability of LSZ as a function of temperature, pH, and denaturing agent (urea).[16,17] Another study in our laboratory showed that the hexagonal structure slowed the transdermal drug (desmopressin) penetration via porcine skin in vitro, compared with the penetration determined via normal aqueous solution. Such lower and better-controlled transdermal transport of the drug opens a number of potential procedures for its sustained release.[18]

In this work, electron paramagnetic resonance (EPR) spectroscopy is used to monitor the loading of insulin into the H_{II} mesophase. EPR analysis by means of spin probes and spin labels specifically added to the systems is well-known to provide precious and unique information about the probe microenvironment, reporting on the distribution of the probes, their mobility and the microviscosity,[19,20] micropolarity,[21] microacidity,[22] and concentration of dissolved oxygen.[23] Furthermore, the technique is noninvasive, providing significant information about the inner microenvironment of the pharmaceutical formulation concerning the accessibility of the drug molecules.[24,25]

Herein, the H_{II} mesophase was investigated for the first time; unloaded and insulin-loaded mesophases were compared utilizing the EPR technique. The microenvironment of H_{II} systems was monitored as a function of temperature and pH using an amphiphilic probe, 5-doxylstearic acid (5-DSA) (Figure 1), which was embedded into the surfactant layer.[26−28] At a high pH (8), 5-DSA probed the surfactant shell closer to the surfactant headgroups, while at a low pH (3) it was closer to the surfactant tails. Hence, these two pH values can also monitor insulin behavior and provide significant information on packing, local mobility, and environmental micropolarity in different microenvironments of the surfactant layer. Studying the structure of the host H_{II} system and the interactions of insulin under temperature-dependent conditions is very important for rational enhancement of its thermal stabilization and controlled release.

2. MATERIALS AND METHODS

2.1. Materials. Monoolein, GMO, distilled glycerol monooleate (min. 97 wt % monoglyceride, 2.5 wt % diglyceride and free glycerol 0.4 wt %; acid value 1.2, iodine value 68.0, melting point 37.5 °C) were obtained from Riken Vitamin Co. (Tokyo, Japan). Tricaprylin (TAG) (97 to 98 wt %) and HCl solution (1.0 N) were purchased from Sigma Chemical Co. (St. Louis, MO, USA). Buffer solution, pH 8.00 (± 0.01 at 25 °C), was purchased from Alfa Aesar (Ward Hill, MA, USA). Insulin human recombinant was obtained from Biological Industries (Beit Ha'emek, Israel). The water was double-distilled. D_2O (D, 99.9%) and DCl solution (D, 99.96%) were purchased from Cambridge Isotope Laboratories, Inc. (Andover, MA, USA). All ingredients were used without further purification.

2.2. Preparation of H_{II} Mesophases. The GMO/TAG/water H_{II} mesophases were prepared by mixing weighed quantities of GMO and TAG (9:1 weight ratio), while heating to 45 °C. This was done in sealed tubes under nitrogen atmosphere to avoid oxidation of the GMO. An appropriate quantity of preheated water (20 wt %) at the same temperature was added, and the samples were stirred and cooled to 25 °C. Empty and insulin-loaded H_{II} systems were prepared at two distinct pH values (3 and 8). At pH 3, 4 wt % insulin was solubilized in water prior to its incorporation into the H_{II} mesophase, while at pH 8 only 0.02 wt % insulin was solubilized in water. D_2O was used for FTIR measurements instead of water. The pH or pD was adjusted to 3 with HCl and DCl, and pH or pD was adjusted to 8 by buffer solution. It should be noted that as a result of insulin solubilization the concentrations of GMO and TAG were decreased, keeping their weight ratio of GMO/TAG (9:1) and water content constant.

2.3. Small Angle X-ray Scattering (SAXS). The existence of the H_{II} mesophase is determined by SAXS measurements, according to Bragg peaks with ratios of d-spacings of $1:1/(3^{1/2}):1/(4^{1/2})$, corresponding to the first three diffraction maxima (h, k = 10, 11, 20) from the 2D hexagonal symmetry. Scattering experiments were performed using Ni-filtered Cu Kα radiation (0.154 nm) from an Elliott rotating anode X-ray generator that operated at a power rating of 1.2 kW. The X-ray radiation was further monochromated and collimated by a single Franks mirror and a series of slits and height limiters and measured by a linear position-sensitive detector. The detector is positioned 0.46 m from the samples. The samples were held in 1.5 mm quartz X-ray capillaries inserted into a copper block sample holder. The temperature was maintained at $T \pm 0.5$ °C with a recirculating water bath. The camera constants were calibrated using anhydrous cholesterol. The scattering patterns were desmeared using the Lake procedure implemented in home-written software.[29] The error reported for the SAXS lattice parameter is ±0.5 Å. It should be stressed that in most measurement based on minimum three different samples the error bar was < ±0.5 Å. The radii of the water cylinders R_W were calculated using the obtained lattice parameter.[16]

2.4. Attenuated Total Reflectance Fourier Transform Infrared (ATR-FTIR) Measurements. An Alpha T model spectrophotometer, equipped with a single reflection diamond ATR sampling module, manufactured by Bruker Optik GmbH (Ettlingen, Germany), was used to record the FTIR spectra. The spectra were recorded with 50 scans, at 25, 40, 60, and 70 °C; a spectral resolution of 2 cm^{-1} was obtained.

2.5. Electron Paramagnetic Resonance (EPR) Measurements. *2.5.1. Insertion of the Probe.* The 5-DSA probe

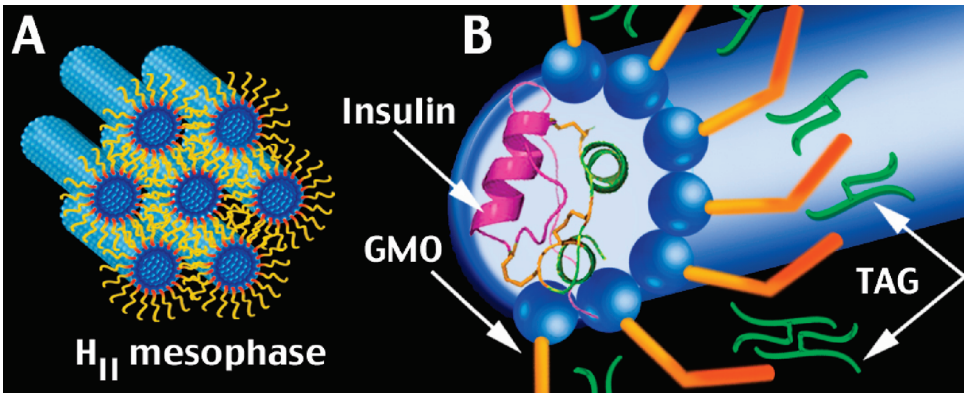

Figure 2. (A) Schematic presentation of the supramolecular organization of the H_{II} mesophase, showing the cylinders packing. (B) Schematic illustration focused on one cylinder of the GMO hexagonal system organization and the localization of insulin within the structure.

(Figure 1) was first dissolved in chloroform at a concentration of 2.5×10^{-3} M as a stock solution. An appropriate quantity of the probe solution was placed in tubes, and the solvent then evaporated before preparing the H_{II} mesophases within these tubes. A low concentration of 1×10^{-4} M probe in the examined H_{II} systems was used for all EPR studies. Such a low concentration has already been demonstrated not to perturb similar nanostructures.[26,27]

2.5.2. Instrumentation and Methods. The spectra were recorded 24 h after sample preparation. Samples were placed in a 20 mm long, 4 mm outer diameter Wilmad EPR quartz tube. EPR measurements with the temperature range of 295.0 K $\leq T \leq$ 343.0 K were carried out using a Bruker EMX-220 X-band ($\nu \sim$ 9.4 GHz) equipped with Bruker ER 4121VT LN_2 temperature accessories and Agilent 53150A frequency counter. EPR experiment setup includes a nonsaturating MW power of 20 mW, a modulation amplitude of 1 G, MW frequency of 9.42 GHz, center magnetic field of 3355.00 G, sweep width of 200.00 G, resolution of 1024 points, time constant of 0.32 ms, and conversion time of 10.24 ms, with a coherent acquisition of 49 scans per each EPR spectrum.

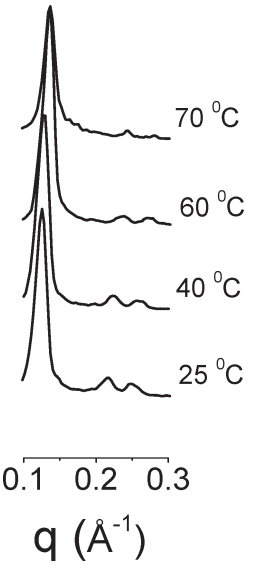

Figure 3. SAXS pattern of the H_{II} mesophase at 25, 40, 60, and 70 °C.

3. RESULTS

In the present study insulin-loaded H_{II} systems were investigated (Figure 2) to characterize the microenvironment of insulin. The microviscosity, micropolarity, and the order of systems in the absence (empty H_{II} systems) and in the presence of insulin were analyzed by EPR as a function of pH by adding 5-DSA (Figure 1) to the mixtures followed by a computer-aided comparative analysis. At pH 8, 5-DSA monitored the GMO shell closer to its headgroups, while at pH 3, the doxyl group was positioned in the vicinity of the GMO tails. Consequently, EPR measurements at these two distinct pH values (3 and 8) characterize different microenvironments within the H_{II} mesophase and also following insulin embedment into the mesophase. Insulin has a very low solubility in water at pH 8, and hence a suitable concentration was used to prevent the formation of hexamers;[30] however, it is soluble in aqueous solution (pH 3), in which the prevalent form of insulin is a dimer. Thus, SAXS diffractions were needed to determine the impacts of insulin and pH on the H_{II} symmetry, geometrical parameters, and boundaries of the liquid crystalline systems. The ATR-FTIR study of the molecular interactions of the protein and the carrier in the acidic (pH 3) H_{II} system was also performed and compared to empty H_{II} systems. All measurements were carried out as a function of temperature.

3.1. Lattice Parameter of H_{II} Mesophase: SAXS Experiment. At first, the two empty H_{II} systems differing in their pH (3 and 8), were examined by SAXS as a function of temperature. SAXS diffractions at a temperature range of 25−70 °C are presented in Figure 3. The diffractions showed that the lattice parameters of the H_{II} systems were similar at both pH values. The measured lattice parameters were 57.7, 56.5, 53.6, and 52.0 ± 0.5 Å at 25, 40, 60, and 70 °C, respectively. Liquid crystalline mesophases are known to be temperature-dependent. Although the hexagonal symmetry remained intact up to 75 °C, the lattice parameter decreased with temperature. The shrinking effect in the lattice parameter is attributed to both the dehydration of the surfactant polar headgroups and to an increase in the hydrocarbon chain mobility, leading to the shortening of the "effective" length of the tails.[14]

At more elevated temperatures (above 75 °C), the H_{II} mesophase disintegrates, and a micellar solution (L_2) is formed in good agreement with previous studies and observations.[13,14,17]

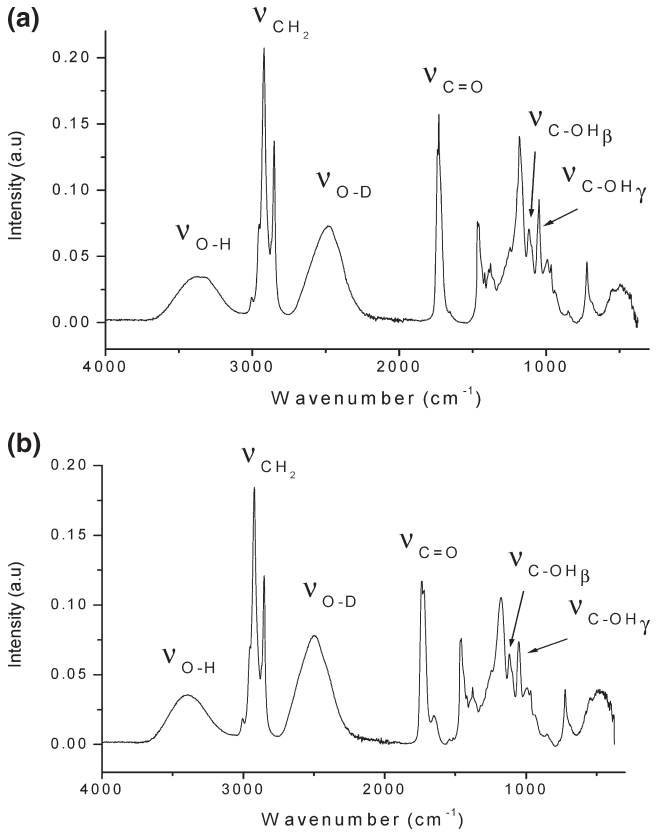

Figure 4. Representative ATR-FTIR spectra of (a) empty and (b) 4 wt % insulin-loaded H_{II} mesophase.

SAXS measurements on insulin-loaded hexagonal structures as a function of pH and temperature were carried out and compared to the empty mesophases. Insulin solubilization under acidic (4 wt % insulin; pH 3) or basic (0.02 wt % insulin; pH 8) conditions did not influence the lattice parameter in the measured temperature range. This indicates that insulin embedment preserves the hexagonal symmetry and geometrical parameters of the H_{II} mesophase. The radius of insulin in its monomeric and dimeric conformations is reported as 11.6 and 14.9 Å, respectively;[31] the hydrodynamic radius was calculated to be 14.5 Å in water.[32] We found that the calculated radii of the H_{II} mesophase containing GMO/TAG/water at a weight ratio of 72:8:20 are 13.2, 13.0, 12.3, and 11.9 ± 0.5 Å at 25, 40, 60, and 70 °C, respectively. The obtained results indicate that the diameter of the cylinders is smaller than the diameter of insulin. Hence it can be proposed that insulin is partially intercalated at the interface region to fit into the narrow water cylinders, as observed and explained in our previous study on lysozyme.[16] Two opposite effects play a role in the solubilization of macromolecules larger than the diameter of the columnar channel: (i) channel swelling due to the embedment of the protein; and (ii) partial dehydration of the hydrophilic heads of GMO which leads to the shrinkage in their diameter. Thus, the net effect was reflected in keeping the lattice dimensions intact.[16]

3.2. Molecular Interactions within H_{II} Mesophase: ATR-FTIR Analysis. ATR-FTIR is a very reliable technique to determine molecular interactions of surfactants, water, and guest molecules. ATR-FTIR spectra analysis of the molecular interactions of the empty H_{II} systems at pH 3 and 8 was recorded at 25, 40, 60, and 70 °C. The resolved vibrational bands are presented in Figure 4a. The vibrational spectra of the two empty H_{II} systems were similar in the entire temperature range. Hence, it can be concluded that the pH of the water cylinders had no effect on the vibration energies of the water molecules within the H_{II} mesophase. This phenomenon may be due to the fact that GMO is a nonionic surfactant, and therefore the variation of proton content in water has a minor effect on the molecular interactions of the H_{II} mesophase.[33]

The molecular (vibrational) interactions of a 4 wt % insulin-loaded system at pH 3 were also investigated as a function of temperature (Figure 4b). However, due to insulin's low solubility at pH 8, the molecular interactions in this basic environment could not be studied. Nevertheless, since pH variation did not affect the lattice parameter of the empty and the loaded H_{II} mesophase (as obtained from SAXS), and since the two empty H_{II} systems at pH 3 and 8 had similar vibrational spectra, we assume that the molecular interactions of the insulin-loaded system at pH 8 would act like those at pH 3.

The structure of the H_{II} mesophases was elucidated using D_2O instead of H_2O to distinguish between the molecular vibrations of the water and the GMO headgroups. The O−D stretching (asymmetric and symmetric) modes and the overtone of bending (υ_{OD}) of the D_2O molecules vibrate at ∼2500 cm^{-1}. At both empty H_{II} mesophases, the position of υ_{OD} showed a visible increase from 2484 cm^{-1} at 25 °C to 2516 cm^{-1} at 70 °C (Table 1). Such an increase in υ_{OD} provides evidence of the weakening of the hydrogen bonding between D_2O molecules upon heating. When insulin was solubilized in water (pH 3), the υ_{OD} vibration was at 2498 cm^{-1} at 25 °C (Table 1). Such a vibration shift points to the competition of insulin on the hydration water causing breakage of bulk water−hydrogen bonds. Heating of the insulin-loaded sample to 40 and 60 °C also shifts the O−D vibration (υ_{OD}) up to the same energy level as that of the empty mesophase. However, further heating to 70 °C had the opposite down-shift effect to 2508 cm^{-1}. This phenomenon may be related to denaturation of the protein, which loses its tertiary structure and undergoes interprotein stacking and precipitation with the release of the solvating water.[34,35] Hence the hydrogen bonding between D_2O molecules increased.

Additionally, each spectrum was analyzed in two distinct structural regions of the surfactant interactions: (1) GMO headgroups, including its hydroxyl groups facing the inner cylinders containing water, and its carbonyl groups located at the interface; and (2) TAG and GMO tails, the interactions derived from the lipophilic region containing the fatty tails.

The structural region of the H_{II} mesophase corresponds to the water−GMO interface. O−H stretching vibrations (υ_{OH}) of the GMO hydroxyl groups absorb at ∼3400 cm^{-1}. In both empty H_{II} mesophases, υ_{OH} significantly increased from 3397 cm^{-1} at 25 °C to 3432 cm^{-1} at 70 °C (Table 1). This is due to the weakening of the hydrogen bonding between the hydroxyls of GMO and D_2O molecules upon heating. Upon insulin solubilization, υ_{OH} showed a down-shift in the whole measured temperature range (Table 1). Hence insulin embedment within the H_{II} mesophase increased the hydrogen bonding between GMO hydroxyls and GMO environment, which includes D_2O and insulin. In addition, hydroxyl stretching vibrations (υ_{C-OH} (β) ∼ 1117 cm^{-1} and υ_{C-OH} (γ) ∼ 1051 cm^{-1}), and the carbonyl stretching vibrations [$\upsilon_{C=O}$ ("free") ∼1743 cm^{-1} and $\upsilon_{C=O}$ (hydrogen-bonded) ∼1725 cm^{-1}] did not show any significant

Table 1. O−D Stretching Wavenumber (cm^{-1}) and O−H Stretching Wavenumber (cm^{-1}) as a Function of Temperature in Empty and Insulin-Loaded H_{II} Mesophase at pH = 3

	O−D stretching wavenumber (cm^{-1})		O−H stretching wavenumber (cm^{-1})	
t (°C)	empty	insulin-loaded	empty	insulin-loaded
25	2484	2498	3397	3394
40	2501	2502	3411	3410
60	2514	2514	3425	3413
70	2516	2508	3432	3420

variation as a function of temperature and/or with insulin solubilization. This indicates that insulin, embedded within the cylinders, interacts with the hydroxyl groups, yet does not affect the carbonyl groups located at the interface.

The second spectral region of the H_{II} mesophase is constituted by the methylene symmetric and antisymmetric stretching vibrations (υ_{CH_2}) of GMO and TAG tails at 2853 and 2924 cm^{-1}, respectively. The C═CH stretching vibration ($\upsilon_{C=CH}$) of GMO absorbs at 3001 cm^{-1}. No changes were detected from the empty to the loaded H_{II} mesophases or by changing temperature in the whole temperature range. Therefore, it can be concluded that neither temperature nor the embedment of insulin has an impact on the hydrophobic region since its location is isolated from this area.[36]

Both SAXS and ATR-FTIR results indicate that the structure of the H_{II} mesophase investigated in this study was not influenced by pH variations. To better understand the structural properties of the empty and insulin-loaded H_{II} mesophases, a computer-aided EPR analysis was performed as a function of pH and temperature.

3.3. Microviscosity, Micropolarity, and Order of H_{II} Mesophase: EPR Study. The structure of the H_{II} mesophase depends on physicochemical factors, including surfactant and cosurfactant structure, surfactant and water concentrations, and temperature. The EPR study by means of the 5-DSA spin probe provides useful information about microviscosity, micropolarity, and the order of those systems. The probe's amphiphilic characteristic enables its localization between surfactant molecules reporting on the nearby environment of different structures. The 5-DSA probe is found to be affected by pH variations; that is, at low pH it is un-ionized, whereas at high pH deprotonation occurs.[26,27] Hence, at low pH, the interactions between water molecules and the carboxylic end of the probe are relatively weak (dipole−dipole) leading to a small hydration shell. As a result the doxyl group, located at position five of the stearic chain, senses the hydrophobic environment of the surfactant tails. On the other hand, at high pH values the probe is in the fully ionized form. Thus, there are strong interactions between the water molecules and the carboxylate ion. Consequently, the hydration shell is large, and the doxyl group is located in the well-packed structure, below the polar surfactant heads.

3.3.1. Empty H_{II} Mesophase. The EPR spectra of 5-DSA in solution are constituted by the three hyperfine lines (due to the hyperfine coupling between the unpaired electron spin, $S = 1/2$, and the ^{14}N nitrogen nuclear spin, $I = 1$) at almost the same intensities. When the probe inserts in a viscous environment, the spectral line shape changes, and the analysis needs the use of a computational procedure which takes into account the relaxation process and the different interactions of the magnetic components. The computer-aided analysis of the EPR spectral line shape was performed by means of the well-established procedure of Budil et al.[37] and Schneider and Freed.[38] The g_{ii} component of the **g** tensor for the coupling between the electron spin and the magnetic field were assumed to be equal to $g_{ii} = 2.009$, 2.006, and 2.003, as already done in previous studies for the same probe.[26,27] The parameters which were changed in the calculation to provide the best fitting between the experimental and the computed line shapes were those which were found to monitor the structural and dynamic modifications of the 5-DSA environment in the different experimental conditions well, that is: (a) the A_{ii} components of the **A** tensor for the coupling between the electron spin and the nitrogen nuclear spin, which monitors the variation in the environmental micropolarity of the probes. For a better comparison among the spectra, the averaged hyperfine coupling constant, $\langle A_N \rangle = (A_{xx} + A_{yy} + A_{zz})/3$ is reported. Indeed, in several cases the variations of $\langle A_N \rangle$ were quite small, but we mainly considered these variations, when well reproducible, in terms of trends of polarity variations. (b) The correlation time for the rotational motion (τ). This parameter increased with the decrease in 5-DSA mobility, that is, with the increase in the microviscosity of the probe-environment. A Brownian rotational diffusional model was used, for which $\tau = 1/6D$, where D is the rotational diffusion coefficient. In this case, as already found in previous studies,[26,27,39] the computation is not affected by the anisotropy of motion, and therefore, $\tau_{perp} = \tau_{par} = \tau$ is assumed. In some cases the variations in the τ values were quite small, just above the accuracy (2%) for this parameter, but we mainly trusted the trends of variation of this parameter, when completely reproducible; (c) when the probes are inserted in an ordered lipid layer, the order parameter (S) extracted from simulation monitors the order degree, being $S = 0$ for a completely disordered system and $S = 1$ for an ordered one. (d) When two components characterized by different structural and magnetic parameters contributed to the signal, a subtraction procedure between spectra is able to extract each component, and then a simulation of each was performed to obtain the magnetic and mobility parameters. Double integration of the components provided the relative intensities, measured as the percentage of each component with respect to the overall spectral intensity. These percentages provided the distribution of probes in different microenvironments. Finally, the addition of the simulated components at their relative percentages provided the simulation of the experimental spectrum.

The accuracy of the parameters (2−3%) was determined by simulation: the variation of a parameter larger than 3% led to a perceptible variation of the simulated line shape, and, consequently, to a worse fit between the simulated and the experimental spectrum.

Of course other sets of parameters could provide an equivalent or even better fitting between the experimental and simulated line shapes; but from several attempted computations, the ones reported are the most confident for the physical meaning of the systems.

The experimental and simulated EPR spectra of H_{II} mesophase in acidic medium (pH 3) as a function of temperature are presented in Figure 5. The mobility (τ), order parameters (S), and hyperfine coupling constant ($\langle A_N \rangle$) obtained from simulation are reported in Table 2. At 23 °C, both $\tau = 0.71$ ns and $S = 0.30$ indicate a quite fluid but partially ordered environment of the probe, similar to that found for 5-DSA in dodecylamine (DDA) liquid crystals in the presence of ethanol as fluidificant.[38]

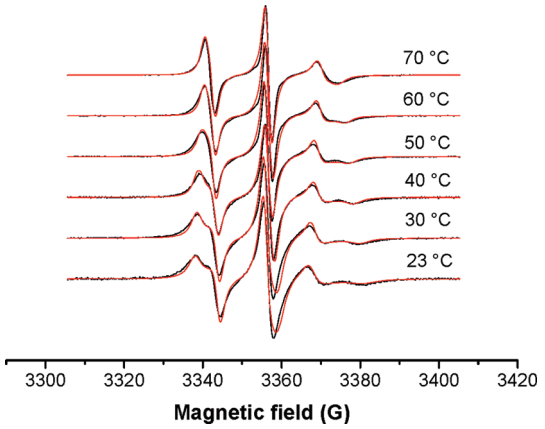

Figure 5. EPR experimental (black lines) and computed (red lines) spectra of H_{II} mesophase in acidic conditions (pH = 3) and at various temperatures.

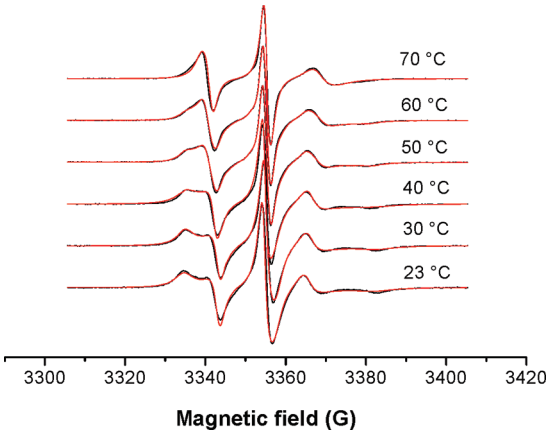

Figure 6. EPR experimental (black lines) and computed (red lines) spectra of H_{II} mesophase in basic conditions (pH = 8) and at different temperatures.

Table 2. Hyperfine Coupling Constant $<A_N>$, Mobility (τ), and Order (S) Parameter Obtained from the Computation of the EPR Spectra of H^{II} Mesophase in Acidic Conditions (pH = 3) and at Various Temperatures[a]

t (°C)	$<A_N>$ (G)	τ (ns)	S
23	15.2	0.71	0.30
30	15.0	0.47	0.30
40	15.0	0.42	0.24
50	15.0	0.33	0.19
60	15.0	0.26	0.15
70	14.9	0.26	0.10

[a] Parameter accuracy: 2%.

Table 3. Hyperfine Coupling Constant $<A_N>$, Mobility (τ), and Order (S) Parameter Obtained from the Computation of the EPR Spectra of H^{II} Mesophase in Basic Conditions (pH = 8) and at Various Temperatures[a]

t (°C)	% component	$<A_N>$ (G)	τ (ns)	S
23	100	15.2	2.10	0.38
30	100	15.2	1.87	0.38
40	100	15.7	1.83	0.33
50	70	15.7	1.83	0.33
	30	15.2	1.83	0.10
60	40	15.7	1.83	0.33
	60	15.2	1.83	0.10
70	100	15.2	1.83	0.10

[a] Parameter accuracy: 2%.

Additionally, the micropolarity, tested by the hyperfine coupling constant $<A_N>$, is also relatively low, indicating that the nitroxide group is localized in a hydrophobic environment. Those results matched the fact that the probe senses the hydrophobic environment of the surfactant tails.

When temperature increased, both τ and S decreased (τ = 0.26 ns and S = 0.10; at 70 °C), indicating decreasing microviscosity and lipid layer order over temperature. This decrease is not linear, and it does not follow a logarithmic variation, thereby indicating that the process involved in the probe rotation in the medium is not a simple one-step process. A close examination of the data also reveals that τ decreased from 0.71 ns at 23 °C to 0.47 ns at 30 °C, while S remained intact. Those results demonstrate that, although there was no order modification, the hydrocarbon chain mobility increases at 30 °C, the temperature at which the dehydration of the headgroup begins.[14] It should be noticed that ATR-FTIR measurements were not sensitive enough to reveal the thermal modification at the GMO tail region.

EPR spectra of H_{II} mesophase in basic conditions (pH 8) as a function of temperature are presented in Figure 6, and the computed parameters ($<A_N>$, τ, S) are listed in Table 3. The computed parameters for this basic system are higher than for the acidic system. These results mean a higher order and microviscosity, due to insertion of the probe in more packed surfactants, as we previously found for 5-DSA in pure DDA liquid crystals.[38] But in the present case a higher micropolarity attests to deprotonation of the COOH group and its approach to other polar-charged groups.

By increasing temperature, microviscosity and order decrease (from τ = 2.10 ns and S = 0.38 at 23 °C, to τ = 1.83 ns and S = 0.10 at 70 °C). Here, again, from 23 to 30 °C microviscosity decreased (from τ = 2.10 ns to τ = 1.87 ns), while S was unchanged. Further analysis of the spectra revealed that at 50 and 60 °C the spectra are clearly constituted by two components, the one at 40 °C and that at 70 °C, at different relative percentages. From 40 to 70 °C the percentage of the spectrum at 70 °C gradually increases at the expenses of the one at 40 °C. This means that the probe is distributed in two different environments that are slowly equilibrating (in the EPR time scale) at 50 and 60 °C, whereas the system is almost homogeneous at the lower and the higher temperatures. Hence it can be assumed from these two distinct populations of the probe that the heating and melting processes of the H_{II} mesophase occur in an ordered way.

3.3.2. Insulin-Loaded H_{II} Mesophase. EPR spectra of insulin-loaded H_{II} mesophase in acidic medium (pH 3) as a function of temperature are presented in Figure 7, and the parameters obtained from simulation ($<A_N>$, τ, S) are summarized in Table 4. The spectra and the computed parameters of the loaded system (pH 3) show the same trends as a function of temperature, as those of the empty systems. At acidic conditions the probe is located close to the GMO tails. Hence, the presence of

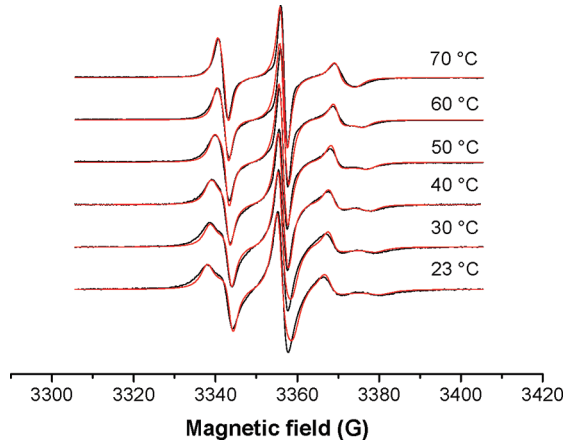

Figure 7. EPR experimental (black lines) and computed (red lines) spectra of insulin-loaded H_{II} mesophase in acidic conditions (pH = 3) and at various temperatures.

Table 4. Hyperfine Coupling Constant $<A_N>$, Mobility (τ), and Order (S) Parameter Obtained from the Computation of the EPR Spectra of Insulin-Loaded H^{II} Mesophase in Acidic Conditions (pH = 3) and at Various Temperatures[a]

t (°C)	$<A_N>$ (G)	τ (ns)	S
23	14.9	0.67	0.30
30	15.0	0.42	0.30
40	15.0	0.42	0.24
50	15.0	0.33	0.19
60	15.0	0.26	0.15
70	14.8	0.26	0.10

[a] Parameter accuracy: 2%.

protein at the interface region would probably be, as expected, insignificant. Yet, insulin embedment into the H_{II} mesophase slightly but not negligibly decreased the microviscosity and polarity of the probe (τ = 0.67 ns and $<A_N>$ = 14.9 G in the loaded system; τ = 0.71 ns and $<A_N>$ = 15.2 G in the empty system, at 23 °C), with the order unchanged. Figure 8 shows in enlarged scale a section of the EPR experimental spectra of empty and insulin-loaded H_{II} mesophase in acidic conditions (pH = 3) at 23 °C, superimposed to highlight the small but not negligible differences between the spectra. The slight increase in mobility can be explained by insulin intercalation, which perturbs the lipid structure. To fit into the narrow water cylinders the protein "pushes aside" the un-ionized 5-DSA probe. Hence the doxyl group, located at position five of the stearic chain, is now compressed even more into the lipophilic region, leading to a mobility increase and a micropolarity decrease.

By increasing the pH to 8, the insulin effect is much more evident. If we compare the EPR results for the insulin-loaded pH 8 system (Figure 9; the main parameters used for computation are reported in Table 5) with those for the empty H_{II} at the same pH (Figure 6 and Table 3), we see how insulin, which interacts with hydroxyl groups of GMO in the outer interface region, perturbs the structure. This leads to a well-defined partition of the probes in two differently structured zones of the system, corresponding to two different spectral components. This partition is also present in the absence of insulin, but the two zones are well-distinguished only in the temperature range of 50−60 °C.

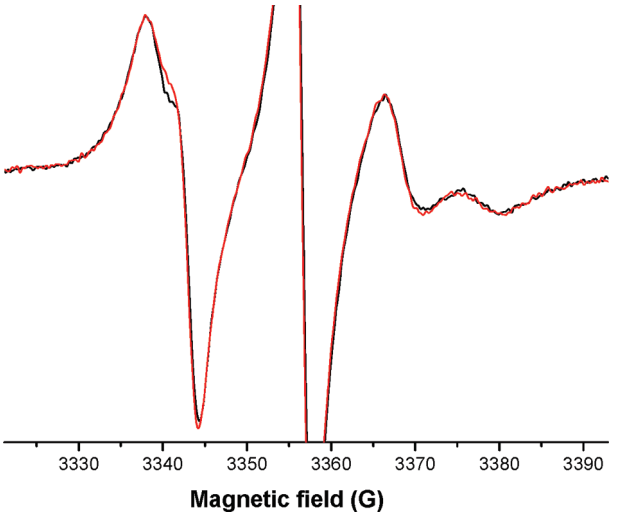

Figure 8. Enlarged scale of a section of the EPR experimental spectra of empty (black line) and insulin-loaded (red line) H_{II} mesophase in acidic conditions (pH = 3) at 23 °C, superimposed to highlight the small but not negligible differences between the spectra.

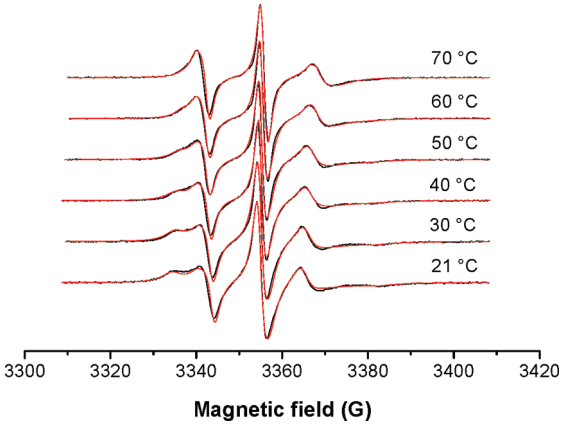

Figure 9. EPR experimental (black lines) and computed (red lines) spectra of insulin-loaded H_{II} mesophase in basic conditions (pH = 8) and at various temperatures.

Conversely, in the presence of insulin, a less ordered and less polar zone is already found at room temperature. Furthermore, while in the absence of insulin the two spectral components are not modified by increasing the temperature and we can reproduce the spectra at 50 and 60 °C by superposition of the spectra at 40 and 70 °C, in the presence of insulin the two components are significantly modified by increasing temperature. In conclusion, the main structural changes in the presence of insulin are: (a) a progressive decrease in order and microviscosity for both the components; (b) a progressive increase in micropolarity, mainly for the less ordered component (from 12.8 at 23 °C to 14.2 at 70 °C), but the micropolarity for this component (on the basis of the calculation) is much lower than that obtained in the absence of insulin. Such results demonstrate how insulin provokes a disordering of the lipid layer leading to multienvironments of the probe. Therefore, in contrast with the empty H_{II} system, the heating and melting processes of the H_{II} mesophase occur in a less ordered way. Consequently, by increasing temperature, the

Table 5. Hyperfine Coupling Constant $<A_N>$, Mobility (τ), and Order (S) Parameter Obtained from the Computation of the EPR Spectra of Insulin Loaded H^{II} Mesophase in Basic Conditions (pH = 8) and at Various Temperatures[a]

t (°C)	% component	$<A_N>$ (G)	τ (ns)	S
23	76	15.0	2.10	0.40
	24	12.8	2.10	0.27
30	76	15.0	2.10	0.37
	24	13.0	2.10	0.21
40	64	15.2	2.10	0.31
	36	13.3	2.10	0.20
50	61	15.2	2.05	0.29
	39	13.8	2.05	0.15
60	46	15.2	1.67	0.29
	54	14.0	1.55	0.14
70	16	15.2	1.67	0.27
	84	14.2	1.48	0.14

[a] Parameter accuracy: 2%.

improved fluidity of the system allows the nitroxide group of the probe to dynamically approach the less hydrophobic lipid regions, and therefore, the micropolarity increases. A close examination of the results (Table 3) reveals that from 50 to 70 °C, both the empty and the loaded systems have the same micropolarity ($<A_N>$ = 15.2 G). This equivalency indicates a similar location of the probe, in agreement with SAXS measurements, which attest that the H_{II} structure is not modified with insulin solubilization. Nevertheless, S increases in the presence of insulin (S = 0.29 and 0.10 in the presence and absence of insulin, respectively). This is in agreement with ATR-FTIR results, which indicate that insulin increases the hydrogen bonding of GMO hydroxyls with its environment in the outer interface region. This increase inhibits the thermal dehydration, leading to an increase in order. Similar behavior was already observed using rheology measurements in the case of lysozyme solubilization within the H_{II} mesophase. Lysozyme incorporation increased the elastic properties and pronounced solid-like response of the systems.[16]

Another interesting trend is the drop in microviscosity. Up to 50 °C the microviscosity of the probe-environment slightly decreased (from 2.10 ns at 23 °C to 2.05 ns at 50 °C); however, at 60 °C the microviscosities of the two components dropped (1.67 and 1.55 ns) and were even lower than in the empty system. At 70 °C there was another slight decrease in microviscosity of one of the components while the second did not change. This means that at elevated temperature the mobility of the probe within the insulin-loaded system was greater than within the empty system. Oppositely, it was found that insulin inhibits the thermal dehydration, and the order parameter increases. To overcome this apparent contradiction, we must consider the protein structure. At high temperature proteins lose their tertiary structure and then aggregate. Insulin is a very sensitive protein that easily aggregates (even at room temperature). Hence the drastic change in microviscosity at 60 °C is attributed to the insulin tertiary structure modifications. Such structural modification of insulin would probably affect its microenvironments and can be followed by an increase in the probe mobility. On this basis, the progressive changes of the two different spectral components may be explained by the unfolding/denaturation process of the protein as a function of temperature.

4. CONCLUSIONS

To study the insulin microenvironment within the H_{II} mesophase, the structure of the carrier and its interactions with insulin under temperature-dependent conditions were investigated using SAXS, ATR-FTIR, and EPR studies. It was seen from SAXS results that insulin entrapment preserved the hexagonal symmetry and the geometrical parameters of the H_{II} mesophase, although its diameter is larger than the diameter of the H_{II} cylinders. An examination of the molecular interaction within the system (ATR-FTIR) implied that insulin embedded in the interface region to fit inside the narrow water cylinders. Insulin interacts with hydroxyl groups of GMO in the outer interface region, implying stronger hydrogen bonding between the surfactant and its environment, which includes water and insulin.

The EPR parameters, microviscosity, micropolarity, order of systems, and distribution of the probes in different microenvironments were influenced by three factors: temperature, pH, and insulin solubilization. Using the amphiphilic spin probe (5-DSA), different microenvironments within the H_{II} mesophase were characterized at two distinct pH values (3 and 8). As expected, at pH 3 the nitroxide group of the probe was localized in a hydrophobic environment, while at pH 8 the probe inserted in the interface, where the microviscosity, order, and micropolarity are greater. When temperature is increased, both microviscosity and order parameters decreased at pH 3 and 8, yet the systems had different decreasing trends. It can be inferred from the results that, in the lipophilic region (pH 3), the microenvironment modifies gradually but not following a one-step process. At the interface (pH 8), there is a gradual change up to 50 °C, in which two processes take place until one of them disappears at 70 °C.

When insulin was incorporated within the H_{II} mesophase, the microviscosity, order, and micropolarity at the lipophilic area (pH 3) slightly decrease compared to the empty system, indicating that the protein perturbs the lipid structure while "pushing aside" the un-ionized 5-DSA probe. The effect of insulin at the interface region (pH 8) is much more evident, presenting two components that are significantly modified by increasing temperature. There was a progressive decrease in order and microviscosity for both the components and a progressive increase in the micropolarity. Results demonstrate how insulin provokes a disordering of the lipid layer leading to multienvironments of the probe within the interface. At high temperatures, the EPR analyses also monitor the unfolding/denaturation process of the protein.

Understanding insulin behavior in the liquid crystalline mesophase assists us in designing vehicles for transdermal delivery of this very important protein. Characterization of the thermal behavior of the insulin-loaded H_{II} system is required, especially in the case of proteins and temperature-dependent systems.

AUTHOR INFORMATION

Corresponding Author

*Tel.: +972-2-658-6574/5; +39-0722-304320. Fax: +972-2-652-0262; +39-0722-304222. E-mails: garti@vms.huji.ac.il; maria.ottaviani@uniurb.it.

REFERENCES

(1) Babiker, A.; Datta, V. *Arch. Dis. Child.* **2011**, *96*, 101–102.
(2) Frid, A.; Hirsch, L.; Gaspar, R.; Hicks, D.; Kreugel, G.; Liersch, J.; Letondeur, C.; Sauvanet, J. P.; Tubiana-Rufi, N.; Strauss, K. *Diabetes Metab.* **2010**, *36*, S3–S18.
(3) Gowthamarajan, K.; Kulkarni, G. *Resonance* **2003**, *8*, 38–46.

(4) Brange, J.; Völund, A. *Adv. Drug Delivery Rev.* **1999**, *35*, 307–335.
(5) Henkin, R. I. *Nutrition* **2010**, *26*, 33–39.
(6) Yadav, N.; Morris, G.; Harding, S. E.; Ang, S.; Adams, G. G. *Endocr. Metab. Immunol. Disord. Drug Target.* **2009**, *9*, 1–13.
(7) Owens, D. R. *Nature Rev.* **2002**, *1*, 529–540.
(8) Rastogi, R.; Anand, S.; Dinda, A. K.; Koul, V. *Drug. Dev. Ind. Pharm.* **2010**, *36*, 993–1004.
(9) Mitragotri, S.; Blankschtein, D.; Langer, R. *Science* **1995**, *269*, 850–853.
(10) Goebel, A.; Neubert, R. H. H. *Skin Pharmacol. Physiol.* **2008**, *21*, 3–9.
(11) Seki, T.; Kluchi, T.; Seto, H.; Kimura, S.; Egawa, Y.; Ueda, H.; Morimot, Y. *Biol. Pharm. Bull.* **2010**, *33*, 1915–1918.
(12) Amar-Yuli, I.; Libster, D.; Aserin, A.; Garti, N. *Curr. Opin. Colloid Interface Sci.* **2009**, *14*, 21–32.
(13) Amar-Yuli, I.; Garti, N. *Colloids Surf., B* **2005**, *43*, 72–82.
(14) Amar-Yuli, I.; Wachtel, E.; Shalev, D. E.; Moshe, H.; Aserin, A.; Garti, N. *J. Phys. Chem.* **2007**, *111*, 13544–13553.
(15) Libster, D.; Ben-Ishai, P.; Aserin, A.; Shoham, G.; Garti, N. *Langmuir* **2008**, *24*, 2118–2127.
(16) Mishraki, T.; Libster, D.; Aserin, A.; Garti, N. *Colloids Surf., B* **2010**, *75*, 47–56.
(17) Mishraki, T.; Libster, D.; Aserin, A.; Garti, N. *Colloids Surf., B* **2010**, *75*, 391–397.
(18) Libster, D.; Aserin, A.; Yariv, D.; Shoham, G.; Garti, N. *Colloids Surf. B* **2009**, *74*, 202–215.
(19) Grammenos, A.; Mouithys-Mickalad, A.; Guelluy, P. H.; Lismont, M.; Piel, G.; Hoebeke, M. *Biochem. Biophys. Res. Commun.* **2010**, *398*, 350–354.
(20) Wilk, K. A.; Zielinska, K.; Jezierski, A. *Colloids Surf., A* **2009**, *343*, 64–69.
(21) Strehmel, V.; Rexhausen, H.; Strauch, P.; Gornitz, E.; Strehmel, B. *Chem. Phys. Chem.* **2008**, *9*, 1294–1302.
(22) Kroll, C.; Herrmann, W.; Stosser, R.; Borchert, H. H.; Mader, K. *Pharm. Res.* **2001**, *18*, 525–530.
(23) Swartz, H.; Khan, N.; Buckey, J.; Comi, R.; Gould, L.; Grinberg, O.; Hartford, A.; Hopf, H.; Hou, H.; Hug, E.; Iwasaki, A.; Lesniewski, P.; Salikhov, I.; Walczak, T. *NMR Biomed.* **2004**, *17*, 335–351.
(24) Kempe, S.; Metz, H.; Mader, K. *Eur. J. Pharm. Biopharm.* **2010**, *74*, 55–66.
(25) Lurie, D. J.; Mader, K. *Adv. Drug Delivery Rev.* **2005**, *57*, 1171–1190.
(26) Kogan, A.; Rozner, S.; Mehta, S.; Somasundaran, P.; Aserin, A.; Garti, N.; Ottaviani, M. F. *J. Phys. Chem. B* **2009**, *113*, 691–699.
(27) Rozner, S.; Kogan, A.; Mehta, S.; Somasundaran, P.; Aserin, A.; Garti, N.; Ottaviani, M. F. *J. Phys. Chem. B* **2009**, *113*, 700–707.
(28) Zuev, Y. F.; Vylegzhanina, N. N.; Zakhartchenko, N. L. *Appl. Magn. Reson.* **2003**, *25*, 29–42.
(29) Lake, J. A. *Acta Crystallogr.* **1967**, *23*, 191–194.
(30) Hvidt, S. *Biophys. Chem.* **1991**, *39*, 205–213.
(31) Nielsen, L.; Khurana, R.; Coats, A.; Frokjaer, S.; Brange, J.; Vyas, S.; Uversky, V. N.; Fink, A. L. *Biochemistry* **2001**, *40*, 6036–6046.
(32) Grudzielanek, S.; Jansen, R.; Winter, R. *J. Mol. Biol.* **2005**, *351*, 879–894.
(33) Kedari, C. S.; Pandit, S. S.; Tripathi, S. C. *J. Membr. Sci.* **2009**, *341*, 122–130.
(34) Kwon, Y. M.; Baudys, M.; Knutson, K.; Kim, S. W. *Pharm. Res.* **2001**, *18*, 1754–1759.
(35) Sivakumar, S.; Wark, K. L.; Gupta, J. K.; Abbott, N. L.; Caruso, F. *Adv. Funct. Mater.* **2009**, *19*, 2260–2265.
(36) Snyder, R. G.; Strauss, H. L.; Elliger, C. A. *J. Phys. Chem.* **1982**, *86*, 5145–5150.
(37) Budil, D. E.; Lee, S.; Saxena, S.; Freed, J. H. *J. Magn. Reson. A* **1996**, *120*, 155–189.
(38) Schneider, D. J.; Freed, J. H. Slow motional magnetic resonance spectra: a user's guide. In *Biological Magnetic Resonance*; Berliner, L. J., Reuben, J., Eds.; Plenum Press: New York, 1989; Vol. 8, pp 1−76.
(39) Galarneau, A.; Sartori, F.; Cangiotti, M.; Mineva, T.; Di Renzo, F.; Ottaviani, M. F. *J. Phys. Chem. B* **2010**, *114*, 2140–2152.